Distribution of peak shear stress in finite element models of reinforced concrete slabs

Lantsoght, Eva; de Boer, A.; van der Veen, Cor

DOI
10.1016/j.engstruct.2017.07.005

Publication date
2017

Document Version
Accepted author manuscript

Published in
Engineering Structures

Postprint of Engineering Structures
Volume 148, 1 October 2017, Pages 571–583
Link to formal publication (Elsevier): https://doi.org/10.1016/j.engstruct.2017.07.005

Highlights (for review)
Click here to download Highlights (for review): highlights distribution shear stress 2015-05-11.docx

- The principle of Levels of Approximation from the *fib* Model Code is applied to assessment, resulting in Levels of Assessment.
- This paper focuses on Level of Assessment II for reinforced concrete slab bridges, for which the shear stress distribution at the support is studied.
- An experiment is compared with a finite element model to come up with a recommendation for the distribution of the peak shear stress in finite element models.
- The recommended width for the distribution is 4 times the effective depth to the longitudinal reinforcement.
- A case study has been made to compare the results of Level of Assessment I and II, and the increased accuracy and reduced conservativism for the higher Level of Assessment is confirmed.

***Abstract**

Click here to download Abstract: abstract distribution shear stress 2015-05-11.docx

Existing reinforced concrete solid slab bridges in the Netherlands are re-assessed for shear based on a Unity Check: the ratio of the shear stress caused by the applied loads to the shear capacity of the concrete cross-section. The governing shear stress resulting from the self-weight, weight of the wearing surface, distributed and concentrated live loads can be determined with a simplified spreadsheet-based method, the Quick Scan (Level of Assessment I) as well as with a linear finite element model (Level of Assessment II). When a finite element model is used, a distribution of shear stress over the width of the slab bridge is automatically found. To compare the governing shear stress caused by the loads to the shear capacity, it is necessary to determine over which length the peak shear stress from the finite element model can be distributed. To answer this question, a finite element model is compared to an experiment. The experiment consists of a continuous, reinforced concrete slab subjected to a single concentrated load close to the support. Seven bearings equipped with load cells that measure the reaction force profile along the width of the slab are used to compare to the stress profile obtained from the finite element model. From this analysis, it is found that the peak shear stress in a linear finite element model can be distributed over $4d_l$ with d_l the effective depth to the longitudinal reinforcement of the slab. The comparison of measured reaction force profiles over the support to the stress profile from a finite element model results in a research-based distribution width that replaces the rules of thumb that were used until now.

Distribution of peak shear stress in finite element models of reinforced concrete slabs

Eva O.L. Lantsoght[a,b] (E.O.L.Lantsoght@tudelft.nl Tel: +593 2 297-1700 ext. 1186 Corresponding Author), Ane de Boer[c] (ane.de.boer@rws.nl), Cor van der Veen[b] (C.vanderveen@tudelft.nl)

[a]Universidad San Francisco de Quito, Politecnico, Diego de Robles y Vía Interoceánica, Quito, Ecuador

[b]Delft University of Technology, Concrete Structures, Stevinweg 1, 2628 CN Delft, The Netherlands

[c]Ministry of Infrastructure and the Environment, Griffioenlaan 2, 3526 LA Utrecht, The Netherlands

Abstract

Existing reinforced concrete solid slab bridges in the Netherlands are re-assessed for shear based on a Unity Check: the ratio of the shear stress caused by the applied loads to the shear capacity of the concrete cross-section. The governing shear stress resulting from the self-weight, weight of the wearing surface, distributed and concentrated live loads, can be determined with a simplified spreadsheet-based method, the Quick Scan (Level of Assessment I) as well as with a linear finite element model (Level of Assessment II). When a finite element model is used, a distribution of shear stresses over the width of the slab bridge is automatically found. To compare the governing shear stress caused by the loads to the shear capacity, it is necessary to determine over which width the peak shear stress from the finite element model can be distributed. To answer this question, a finite element model is compared to an experiment. The experiment consists of a continuous, reinforced concrete slab subjected to a single concentrated load close to the support. Seven bearings equipped with load cells that measure the reaction force profile along the width of the slab are used to compare to the stress profile obtained from the finite element model. From this analysis, it is found that the peak shear stress in a linear finite element model can be distributed over $4d_l$ with d_l the effective depth to the longitudinal reinforcement of the slab. The comparison of measured reaction force profiles over the support to the stress profile from a finite element model results in a research-based distribution width that replaces the rules of thumb that were used until now.

Keywords

experiment; finite element models; punching shear; slab; shear; shear stress; structural load test.

1. Introduction

The Dutch road network underwent a large expansion during the decades following the Second World War. Fifty percent of the bridges and viaducts in the Netherlands were built before 1976. The bridges that were constructed at that time are now reaching the end of their originally devised service life. Since the original design and construction of these bridges, the traffic loads and volumes have increased significantly, resulting in heavier live load models in NEN-EN 1991-2:2003 [1]. At the same time, the shear provisions of the recently introduced Eurocode NEN-EN 1992-1-1:2005 [2] allow for smaller shear capacities of concrete cross-sections than the former national Dutch code NEN 3880:1974 [3] and NEN 1009:1962 [4] (or earlier).

One bridge type that, upon assessment, is particularly vulnerable to these code changes is the subset of the reinforced concrete solid slab bridges. This bridge type is common in the older part of the Dutch road network, and is typically used for covering short spans. The number of slab bridges that need further study in the Netherlands is 600. While the calculated cross-sectional shear capacity might be insufficient, these bridges did not show signs of distress upon inspection [5]. This observation indicates that reinforced concrete slabs possess additional sources of capacity that are traditionally not taken into account in the concrete design codes. In slabs, one of the major sources of additional capacity is the slab's ability for transverse load redistribution [6] and the influence of the width of the member [7]. A full literature survey on the shear strength of reinforced concrete slabs [8] and review of experiments available in the literature [9] confirm the increased shear capacity of reinforced concrete slabs as compared to beams [10-13].

This paper deals with the assessment of reinforced concrete slab bridges based on linear finite element models, as part of an approach based on Levels of Approximation. For the first

time, the distribution width of the peak shear stress is studied experimentally, whereas in the past, rules of thumb were used.

2. Levels of Assessment

In the 2010 *fib* Model Code [14], a new concept is introduced for structural engineers: the use of Levels of Approximation, as shown in Figure 1. Increasing the Level of Approximation means using a computational technique that requires more time but that gives results that are expected to be more accurate.

The concept of using Levels of Approximation is used for the analysis of the 600 shear-critical reinforced concrete slab bridges in the Netherlands. The Levels of Approximation for the assessment of bridges are renamed as “Levels of Assessment”. All bridges that are under discussion need to be analyzed with Level of Assessment I. The bridges that fulfil the criteria of Level of Assessment I, or, in other words, when the shear capacity of the cross-section is larger than the shear stress resulting from the applied loads, are not analyzed further. The bridges with one or more cross-sections that do not fulfill the requirements of Level of Assessment I are reanalyzed with Level of Assessment II. As before, the bridges with cross-sections that are found to be sufficient with Level of Assessment II, are not studied further. The bridges with one or more cross-sections that do not fulfill the Level of Assessment II criteria are taken into Level of Assessment III. This procedure is repeated throughout the higher Levels of Assessment.

For assessment of the existing reinforced concrete slab bridges, Level of Assessment I consists of a spreadsheet-based calculation, which is similar to a hand calculation. This approach is called the “Quick Scan” [15, 16]. The shear stress resulting from the acting forces is determined by using superposition of the individual contributions. The shear stress from the distributed loads is determined based on static equilibrium and the shear stress from

concentrated loads is based on a 45^o load distribution in the plane of the slab so that the effective width in shear over which this load is acting can be determined. The shear capacity is determined by NEN-EN 1992-1-1:2005 [2] with a lower bound v_{min} as derived by Walraven [17]. The spreadsheet can read in all information from the database of the bridges under study, and as output it gives the maximum Unity Check (the ratio between the design value of the applied shear stress resulting from the loads (composite dead load and live load) and the shear resistance as prescribed by the Eurocode [2]), of the critical cross-section, per bridge section span. This method allows for a fast identification of which bridges can be considered sufficient and which bridges need further study. A number of conservative assumptions have been made in the Quick Scan: the effective width of the concentrated loads is determined per axle of the design truck, and the same effective width is used for both axles of the design truck (giving a smaller effective width to the second axle than when 45^o load spreading would be applied) [18]. A smaller effective width will result in a larger shear stress for the same applied live load model. Moreover, the larger distributed live load in the first lane with slow truck traffic is distributed over only a small portion of the width, which is a more conservative approach than using a distribution based on Guyon-Massonet [19]. The thickness of the asphalt layer is conservatively assumed to be 12 mm, which leads to larger shear stresses than a smaller layer [18].

For Level of Assessment II a linear finite element model is used to find the governing shear stress caused by the applied loads. A linear elastic finite element model is used in Level of Assessment II instead of a non-linear analysis (Level of Assessment III), which can take cracking and transverse load redistribution into account and provides a more rigorous analysis, because it is less time-consuming and can be sufficient for a number of structures under study. The shear stress caused by the applied loads is compared to the shear capacity of

the cross-section, as defined by NEN-EN 1992-1-1:2005 [2] with a lower bound v_{min} as described by Walraven [17]. The design tandems have to be moved in such a way that the most unfavorable position is found, resulting in the largest possible shear stress for the given loads. The output of the model is the distribution of the shear stress over the width at the support. The peak shear stress in this distribution needs to be averaged over a certain distance to achieve the shear stress that can be compared to the code-prescribed shear capacity. The distribution width is typically determined based on rules of thumb and local practice. In The Netherlands, a multiple of the effective depth to the longitudinal flexural reinforcement, d_l, is used. The recommendations in this paper are developed to be used with a linear finite element program for a Level of Assessment II evaluation and to help engineers identify the governing shear stress.

Higher Levels of Assessment include non-linear finite element models and probabilistic analysis for Level of Assessment III, and proof loading for Level of Assessment IV. These higher levels are outside of the scope of this paper. Guidelines for the use of non-linear finite element models have been developed [20] and have been applied to the discussed slab shear experiments [21]. Proof loading of slab bridges is currently being studied. Preliminary results can be found elsewhere [22-26].

3. Description of experiment

3.1. Test setup

Experiment S25T1 is used for comparison to a linear finite element model to come up with recommendations for the distribution width as a multiple of d_l. This experiment is part of a series of experiments from Delft University of Technology designed to better understand the shear capacity of reinforced concrete slabs under concentrated loads close to supports. In a

first series, 18 slabs and 12 slab strips were tested under a concentrated load close to the support [7, 27] to study the difference in shear behavior between beams and slabs. In a second series, an additional 8 slabs were tested under a combination of a concentrated load close to the support and a line load [28] to verify if the hypothesis of superposition is valid at the ultimate limit state. S25 was a specimen pertaining to the second series of experiments, but during the first experiment on this slab, S25T1, only a single concentrated load was used, which is the loading configuration from the first series of experiments. S25T1 is thus the only experiment with the test setup of the second series, which includes the use of load cells distributed over the support, but with the loading configuration of the first series of experiments. As such, only this single experiment is suitable for the analysis of the distribution width of the concentrated load. Only one test as such is available, as S25T1 was originally carried out to verify that the results and recommendations from the first series are still valid when a slightly different test setup (as used in the second series) was used. The question with regard to the distribution width for application to the second Level of Approximation only arose after carrying out all experiments and dismantling the test setup. Therefore, it was not possible to carry out additional experiments. The reader should keep this limitation in mind.

A sketch of the test setup for S25T1 is shown in Figure 2a and a photograph is given in Figure 2b. The size of the slab was 5 m × 0.3 m × 2.5 m, representing a half-scale continuous solid slab bridge. The span length was 3.6 m.

The line supports consisted of a steel beam (HEM 300 with h = 300 mm) of 300 mm wide, on which 7 steel bearings of 350 mm × 280 mm × 45 mm provided with load cells (or dummy blocks) and hinges were placed. The load cells were used on the support close to which the experiment was carried out, and the other support was equipped with dummy

blocks. On top of the steel bearings, a steel strip of 100 mm × 15 mm × 2500 mm and 7 strips of felt N100 of 100 mm × 5 mm × 280 mm were used. The felt properties of felt type N100 have been tested previously [29] and the compression stiffness was found to be 6.5 Nmm/mm^3.

Three vertical prestressing bars couple the cantilevering end of the slab past support 2 to the laboratory floor (Fig. 2a), creating a moment over support 2 and thus simulating a continuous support (CS) for support 2. The prestressing force is applied at the beginning of every experiment to offset the self-weight of the slab and increases over the course of the experiment. Load cells measure the force in the prestressing bars so that the moment over support 2 is known at all time during the experiment. The prestressing at the beginning of the experiment was 3 × 15 kN.

The size of the loading plate was 300 mm × 300 mm. In S25T1, the load is applied in a displacement-controlled way in the middle of the width, close to the simple support. The center-to-center distance between the load and the support, a, was 600 mm in the experiment, as shown in Fig. 2a.

3.2. Tested specimen

Deformed bars of steel S500 with a diameter of 20 mm and a yield strength f_{ym} = 542 MPa and ultimate strength f_{um} = 658 MPa as well as bars with a diameter of 10 mm and f_{ym} = 537 MPa and f_{um} = 628 MPa were used. The main longitudinal reinforcement of S25 consisted of φ20 mm bars spaced at 125 mm on center, and the transverse flexural reinforcement consisted of φ10 mm bars spaced at 125 mm on center. A concrete cover of 25 mm was used, so that the effective depth to the longitudinal reinforcement equaled d_l = 265 mm. Thus, S25 had a longitudinal reinforcement ratio ρ_l = 0.996% and a transverse flexural reinforcement ratio of ρ_t = 0.258%.

Normal strength concrete class C28/35 with a maximum aggregate size of 16 mm was used. The aggregates were glacial river aggregates. The cube concrete compressive strength at the age of testing (170 days since casting) was $f_{c,cube}$ = 58.6 MPa and the tensile splitting strength was f_{ct} = 4.5 MPa.

3.3. Experimental results

Failure occurred for a maximum concentrated load of P_u = 1461 kN. After the experiment, mostly longitudinal cracks were observed on the bottom of the slab [30], as well as some punching damage. Remarkably, and contrarily to earlier experiments with similar loading conditions [27], on the side faces no cracks were visible, not even flexural cracks.

Laser distance finders were used to instrument the slab and measure the deformations. All measurements can be found in the full test report [30]. The load-displacement diagram of S25T1 and the forces in the prestressing bars are given in Figure 3. In Figure 4, the most important deflection plots of the experiments are given. As can be seen from Figures 3 and 4, the load is applied at a constant rate in a displacement-controlled manner. For the analysis, as discussed in the next paragraph, a few measurement points were isolated to compare at these points with the finite element model.

At the simple support line, the seven load cells were used to measure the reaction force and its distribution over the support width continuously during the experiment. For the current study, nine levels of the continuously increasing applied loading in increments of 10% of the ultimate load (up to 90% of the ultimate load on the slab) are used. The final interval from 90% of ultimate load to 100% of the ultimate load is not considered because the behavior of cracking of the concrete and slipping of the concrete with respect to the reinforcement bar cannot be represented correctly by a linear finite element model. The measured reaction forces in the load cells are graphically represented in Figure 5a. Not all

load cells are activated from the beginning of the experiment because of the small, but significant, geometric imperfections of the reinforced concrete slab that result in the unconnected areas between the slab and the load cells. For future experimental work, it is recommended to use an interface layer between the slab and the support, for example a layer of plaster of Paris, to ensure a better contact between the slab and the support.

4. Finite element model of experiment

4.1. Description of finite element model

The experiment was simulated in Diana, Release 9.4.4 [31]. The supports were modeled as 3D solid elements. Figure 6 shows a rendering of the model with the different elements labelled.

The concrete slab was modelled as shell elements with a Young's modulus of 31.6 GPa in the main direction and 10.5 GPa in the other directions; with a shear modulus of 13.7 GPa in the main direction and 4.6 GPa in the other directions; with a Poison's ratio of 0.15 and with a density of 25 kN/m^3. The Poisson ratio is set to 0.15, according the Dutch guidelines for modelling of concrete [20]. Of course, the Poisson ratio should be reduced when serious cracking occurs, with the reduction in relation to the crack width. Orthotropic behaviour is already foreseen, so reducing the Poisson ratio to zero is more or less double. These analyses are all linear static, and the Poisson reduction is available and highly recommended in nonlinear analysis. Gauss point values for the stresses can be recommended. The slab behaviour simulation by a nonlinear simulation, which is not included in this paper, but can be found elsewhere [21], shows until about 80% of the ULS load, that the Poisson ratio can be set to 0.15. After this 80% ULS criteria some Poisson ratios belonging to severely cracked elements need to be modified.

In between the solid elements and the shell elements, interface elements representing the layer of felt were used. The interface elements have a normal stiffness and shear stiffness. The normal stiffness is calculated as the Young's modulus of the concrete, divided by the thickness of the interface element. The shear stiffness is taken as 1% of the normal stiffness.

The reinforcement bars were modeled as embedded steel bars. For the model, 40% of orthotropy was assumed.

Mapped meshing was used. The FE mesh is set up with the dimension based on the thickness of the slab. The Rijkswaterstaat NLFEA recommendation [20] tells us that the length and width of a single slab element should be less or equal to half of the thickness of the slab. In this way, the problem of missing local forces at the edges of the slab can be avoided. The resulting mesh is shown in Fig. 6b for the top view and Fig. 6c for the side view. The extrapolation to nodal stress values is used and permitted for linear finite element models, whereas this practice is not recommended for nonlinear finite element models.

The load was modeled as a uniformly distributed load applied to a steel plate of 300 mm × 300 mm, as in the experiment. Solid elements were used to model the loading plate. All steel elements had a Young's modulus of 200 GPa and a Poison's ratio of 0.3. In the experiment, the slab was not resting on all bearings due to initial geometric imperfections. Based on the measurements of the reaction forces in the supports (Fig. 5), a phased activation of the supports was implemented into the model.

These choices for modeling results in 42 elements for the width of the slab by 71 elements for the length of the slab. The supports were modeled as steel beams with 2 elements over the height, 2 elements over the width and 42 elements over the length. The interface was modeled as 2 elements over the width and 42 elements over the length. The three prestressing bars were taken into account.

The presented linear finite element model mostly is based on choices that are standard in current engineering practice. However, to study the finite element modeling of reinforced concrete slabs, both the use of solid and plate elements was explored. Additionally, to develop guidelines for the modeling of reinforced concrete slabs, several experiments tested in the Stevin II Laboratory of Delft University of Technology as well as from the literature were modeled with linear and non-linear finite element models [20, 21, 32-34]. Moreover, the required safety format was studied in the cited studies, analyzing both mean values to simulate experiments and the safety format from the *fib* Model Code [14] for the application to the assessment practice. These recommendations form the background for the presented modeling.

4.2. Analysis and verification of model

Before the results of the finite element model can be used for comparison to the experiments, the measured reaction forces at the load cells are used to check if the model represents the experiment satisfactorily. The measured reaction forces as shown in Figure 5a can be compared to reaction forces in the model. The same nine intervals of the applied load are considered. The resulting reaction forces from the model are presented in Figure 5b. The reaction forces in the experiment and model are similar, as can been seen from comparing Figures 3a and b. This observation indicates that the performance of the finite element model is satisfactory and that the model can be used to study the distribution width of the peak shear stresses and formulate a recommendation for the use with Level of Assessment II. The reaction forces over the support are asymmetric as a result of the lack of contact at certain points between the slab and the support. Whereas this experimental observation caused an extra challenge in modeling the slab, it is not expected that the asymmetric support reactions pose a limitation to the results. Moreover, the loading on reinforced concrete slab bridges

according to the Eurocodes for assessment is asymmetric, with the heaviest truck in the first lane [35].

5. Analysis of experimental results

5.1. Results of the experiment

The analysis of the results of the experiment and the linear elastic finite element model aim at comparing the shear stress distributions and formulating recommendations for the distribution width around the peak shear stress in the finite element model. The distribution width will be expressed as a multiple of the effective depth to the longitudinal reinforcement d_l.

First, the measured reaction forces over the width of the slab in experiment S25T1 are analyzed. To carry out the shear stress analysis, the reaction forces need to be converted into shear stresses. This analysis is carried out at two levels of the ultimate load: 40% of the ultimate load or with an applied concentrated load of 585 kN, assuming the Serviceability Limit State (SLS) conditions, and 90% of the ultimate load or with an applied concentrated load of 1314 kN, assuming the Ultimate Limit State (ULS) conditions. The calculation procedure here is illustrated for the case of an applied concentrated load of 1314 kN. Since the reaction forces in the experiment are measured only at seven discrete positions over the slab width, it is assumed that the reaction force is distributed uniformly over the influence length of the support. Because of the geometry, the influence length of the load cells is 358 mm. A sketch of the situation, indicating the distribution over $2d_l$ and $4d_l$ is given in Figure 7 and Figure 8 respectively. The length of $2d_l$ equals 530 mm and the length of $4d_l$ equals 1060 mm. These distances are assumed around the center of the middle load cell (FS3), of which the center line coincides with the center of the width of the slab. For a concentrated load of 1314 kN, the largest reaction force in the experiment was found in bearing FS3. In Figure 7, a

distance of d_l is indicated as the distribution width on each side of the center of FS3. The total width of the slab was 2500 mm, and the distance $2d_l$ goes from x = 985 mm to x = 1515 mm along the width of the slab, as shown in Figure 7. For $4d_l$ the positions are x = 720 mm to x = 1780 mm, as shown in Figure 8.

The total applied reaction force, $F_{tot,2d}$ over $2d_l$ is:

$$F_{tot,2d} = FS3 + \frac{86\text{ mm}}{358\text{ mm}}\left(FS2 + FS4\right) = 580\text{ kN} \tag{1}$$

The shear stress over $2d_l$, τ_{2d}, is found by dividing the force $F_{tot,2d}$ by the area. This area has a height of d_l and a width of $2d_l$:

$$\tau_{2d} = \frac{F_{tot,2d}}{2{d_l}^2} = \frac{580\text{ kN}}{2\left(265\text{ mm}\right)^2} = 4.13\text{ MPa} \tag{2}$$

A similar approach is used to determine the applied reaction force $F_{tot,4d}$ over $4d_l$:

$$F_{tot,4d} = FS3 + \frac{351\text{ mm}}{358\text{ mm}}\left(FS2 + FS4\right) = 739\text{ kN} \tag{3}$$

Similarly, the shear stress τ_{4d} over $4d_l$ can be defined as:

$$\tau_{4d} = \frac{F_{tot,4d}}{4{d_l}^2} = \frac{739\text{ kN}}{4\left(265\text{ mm}\right)^2} = 2.63\text{ MPa} \tag{4}$$

At 40% of the ultimate load (585 kN) the largest reaction force occurs at load cell FS5, as can be observed in Figure 5a, due to the phased activation of the supports. A similar procedure as described for a load of 1341 kN is followed, but now the distribution is considered around the center of load cell FS5. Assuming a distribution width of $2d_l$, a total force $F_{tot,2d}$ = 212 kN is found, resulting in a shear stress τ_{2d} = 1.51 MPa. Assuming a distribution width of $4d_l$, a total force $F_{tot,4d}$ = 244 kN is found, resulting in a shear stress τ_{4d} = 0.87 MPa.

5.2. Results of the finite element model

In a next step, the corresponding shear stresses from the linear finite element model are computed. These stresses are then compared to the results of the experiment as calculated in the previous step to formulate a recommendation for the distribution width. The output of the finite element model allows for different ways of analyzing the results. To obtain the shear stress over the distribution width, the following two methods can be used:

1. Integration of the shear stresses over the considered distribution width to determine the shear force at the support, which is then divided by the distribution width and the effective depth, or
2. Analysis of the distribution of the reaction forces in the discrete supports, in the same way as the experimental results were analyzed (Fig. 7, Fig. 8).

For the first method, the shear stress distribution over the support is analyzed. An example is given in Figure 9, for a concentrated load of 585 kN. In Figure 9, the distance $2d_l$ and $4d_l$ is shown around the center of the slab as well as around the peak value of the stress distribution. For the analysis, the position of the peak value of the stress distribution is used as the center of the uniform stress distribution, as is typically done in practice. Integrating the shear stress obtained in the finite element model over $2d_l$ around the peak shear stress results in τ_{2d} = 1.30 MPa and integrating over $4d_l$ results in τ_{4d} = 1.10 MPa. A similar procedure is followed for 90% of the maximum load, for an applied concentrated load of 1314 kN.

For the second method, the reaction forces at the locations of the load cells in the finite element model are studied. These reaction forces are given in Figure 5b. For a load of 585 kN, the peak reaction force is found in FS4, which differs slightly from the peak position in the experiment in load cell FS5. If the method as described for the measured reaction forces is used around the peak for FS4, then $F_{tot,2d}$ = 196 kN and the shear stress over $2d_l$ is found to

be τ_{2d} = 1.39 MPa. For a distribution over $4d_l$, the total load $F_{tot,4d}$ = 356 kN and the shear stress τ_{4d} = 1.27 MPa. A similar procedure is followed for 90% of the maximum load, for an applied concentrated load of 1314 kN.

5.3. Comparison between experiment and finite element model

The previous paragraphs highlighted the calculations at 40% of the maximum load, for a concentrated load of 585 kN and at 90% of the maximum load, for a concentrated load of 1314 kN. An overview comparing the results in the experiment to those from the finite element model is given in Table 1 for 40% of the ultimate experimental load (585 kN) and 90% of the ultimate load (1314 kN). The results in Table 1 show that distributing the peak shear stress over $4d_l$ gives a conservative estimate of the shear stress in the finite element model as compared to the shear stress based on the reaction forces in the experiment. The experimental shear stress is lower than the shear stress based on the finite element model, so the finite element model results in a conservative estimate of the shear stress due to the applied loads when a distribution width of $4d_l$ is used. The results in Table 1 also show similar results for both approaches to determine the shear stress based on the results in the finite element program: integration of the stress distribution from the model or using the resulting reaction forces at the positon of the bearings in the model.

5.4. Unity Check of experiment

The previous paragraphs all focused on finding the governing shear stress and the width over which the peak of the shear stress profile is to be distributed. For an assessment, the governing shear stress is compared to the shear capacity according to NEN-EN 1992-1-1:2005 [2] with v_{min} as defined by Walraven [17] in order to find the Unity Check and see if the cross-section fulfills the criteria. For S25T1 the shear capacity of the cross-section can be found as:

$$v_{Rd,c} = 0.12k\left(100\rho_l f_{ck}\right)^{1/3} = 0.12\times 1.87\left(0.996\times 28\text{MPa}\right)^{1/3} = 0.68\text{MPa} \quad (1)$$

$$v_{min} = \frac{1.08k^{3/2} f_{ck}^{1/2}}{f_{yk}^{1/2}} = \frac{1.08\times 1.87^{3/2}\times 28^{1/2}}{500^{1/2}} = 0.65\text{MPa} \quad (2)$$

The design shear stress is the maximum of v_{min} and $v_{Rd,c}$ and is thus $v_{Rd,c}$ = 0.68 MPa. This value can be compared to the shear stress over $2d_l$ and $4d_l$, for example at 40% of the experimental ultimate load based on the results from integrating the stresses over the support in the finite element model. The value at 40% is considered to be more representative of the shear stresses that develop based on the loads for which the cross-sections are assessed, because of the large loads that were found in the slab shear experiments. The governing shear stress is then τ_{2d} = 1.30 MPa with distribution over $2d_l$ and τ_{4d} = 1.10 MPa with distribution over $4d_l$. As a result, the Unity Check based on a distribution width over $2d_l$ equals 1.91 and based on a distribution width over $4d_l$ equals 1.62.

The resulting Unity Checks indicate the large inherent conservatism in the code as compared to the experimental result, as noted previously in the slab shear research [27]. Also, the Unity Checks show that using a distribution width over $4d_l$ leads to a smaller underestimation of the capacity, and is thus to be preferred. This observation is an additional benefit of using the $4d_l$ distribution width, but not the governing criterion for the choice of the distribution width.

5.5. Higher Levels of Approximation

For Levels of Approximation III, non-linear finite element models are used. The approach followed based on a non-linear finite element model is different from the approach outlined in this paper based on a linear finite element model, and is also different from the Quick Scan approach. For both methods, the capacity is taken based on the formulas from the code,

whereas the model provides the resulting shear stress caused by the loads. In a non-linear finite element model, a different approach is followed. The load is applied in increments to have a load-controlled situation, or by applying increments of displacement at the load, to have a displacement-controlled situation, which is to be preferred. In each load step, the model runs and it is explored if cracking occurs. If cracking occurs, the stiffness of the model in the cracked elements will be reduced for the next load step. As such, a non-linear finite element model is close to the execution of an experiment, and results in a load-displacement diagram. The material model for the concrete (see Figure 10) this case can then be based on a total strain rotating crack model, with exponential softening in tension and parabolic behavior in compression, with a variable Poisson's ratio, and an increase in compressive strength due to lateral confinement. The material model for the reinforcement is based on hardening plasticity, see Figure 11. For the steel loading plate, a linear elastic behavior can be assumed.

In terms of elements, for the concrete 20-node solid elements are recommended, using five elements over the slab height. For the reinforcement bars, embedded truss elements with two Gauss integration points along the axis of the element are recommended. The prestressing bars can be modeled as 2-node truss elements, and the steel plate can be modeled using 20-node solid elements.

An example of application is shown in Figure 12. The crack strain values are shown at the maximum load. A strip of the slab (isolated only in the post-processing stage) is shown, so that the crack strain values can be studied more closely. It can be seen that the inclined cracking, indicating shear failure can be captured by the non-linear finite element model.

Recommendations for the use of non-linear finite element models for the assessment of reinforced concrete slab bridges are being finalized, and will be published shortly [32].

Upon publication of these guidelines, and the agreement on the procedures, the methods for Level of Assessment III will be applied at a larger scale.

The highest Level of Assessment [36] includes the use of proof load tests [37]. This research is currently being carried out. In these pilot proof load tests, measurements are applied over the width of the support, to verify the distribution width in existing bridges. This topic is currently being evaluated.

6. Case Study

In this paragraph, an example reinforced concrete solid slab bridge is analyzed using the Quick Scan method, Level of Assessment I, as well as using a finite element model, Level of Assessment II, to find the governing shear stress. In the Level of Assessment II approach, the recommended distribution width for the peak shear stress of $4d_l$ is used. For both methods, the analysis of the cross-section is based on the Unity Check, the ratio of the shear stress caused by the applied loads to the shear capacity according to NEN-EN 1992-1-1:2005 [2].

It needs to be noted upfront that one of the differences between the Level of Assessment I method and the Level of Assessment II method is that the Quick Scan approach results in Unity Checks for 3 cross-sections, while the finite element results can be used to verify every cross-section in the studied spans.

The case under study is a reinforced concrete solid slab bridge built in 1959. This bridge has 4 spans, with end spans of 10.1 m and mid spans of 14.4 m and a width of 10 m of which 6 m carries traffic. The depth of the slab varies transversely from 530 mm to 470 mm. The depth varies longitudinally from 550 mm at the supports to 530 mm at mid span. Plain reinforcement bars of steel QR24 with a yield strength of 240 MPa are used. The cover to the reinforcement is 25 mm. The sagging moment reinforcement ratio in the end span is ρ_l =

0.69% and the hogging moment reinforcement ratio at the mid supports is ρ_l = 0.78%. As for all existing slab bridges from The Netherlands owned by the Dutch Ministry of Infrastructure and the Environment of which no test results about the concrete strength are available, the characteristic cylinder compressive strength of the concrete can be assumed as f_{ck} = 35 MPa [38].

For the considered case, the governing cross-section in the Quick Scan is at support 2-3 (close to the mid support in the second span) with a shear stress due to composite dead load and live loads from Load Model 1 at the edge of the support v_{Ed} = 0.68 MPa and a shear capacity $v_{Rd,c}$ = 0.91 MPa (the lower bound shear capacity v_{min} [17] is governing over $v_{Rd,c}$ from NEN-EN 1992-1-1:2005 [2]). These stresses result in a Unity Check value of UC = 0.74.

Consequently, a linear finite element model of the considered bridge is used as a Level of Assessment II method. The slab is modeled as a plate with shell elements. The variable depth in the transverse direction is taken into account, while the variable depth in the longitudinal direction is not considered. The governing shear force in the finite element model is found to be 278 kN/m. For the shear capacity the lower bound of the shear stress v_{min} [17] is again found to be governing for the QR24 steel, and results in V_{min} = 438 kN/m. The resulting Unity Check at the governing section is then UC = 0.63.

This comparison shows that the goal of the finite element model as a higher Level of Assessment than the Quick Scan method to be a more selective assessment tool is met. The Quick Scan is based on a series of conservative assumptions that cover the entirety of all solid slab bridges owned by the Dutch Ministry of Infrastructure and the Environment. For individual cases, the assumptions can often prove to be overly conservative. This observation is reflected by the smaller Unity Check found based on the shear stress from the finite

element model, and is according to the philosophy of the Levels of Approximation as shown in Figure 1.

7. Discussion

In experiment S25T1 a flat slab is supported by steel bearings equipped with load cells and hinges. This support condition is different from the practical case of existing solid slab bridges. In a real bridge, an edge beam is often cast onto the slab, which results in an even better distribution of the load over the support. In this experiment, the setup with load cells and hinges was used to study the distribution of the reaction forces at the support. However, because of the use of a line of bearings, the resulting support condition is almost equal to a line support. It however is not cast integrally to the slab, which reduces the transverse distribution capacity. The recommendation of the distribution width to be $4d_l$ based on the comparison between the experiment and the finite element model is thus a conservative approach.

For the modeling of an existing bridge with a linear finite element model, the use of shell elements for the edge beam, instead of 3D solid elements for the support as used in this study, is sufficient. This study used 3D solid elements to model the particular support layout used in the experiment to determine the reaction forces over the width of the slab.

In experiment S25T1, no (flexural) cracks were observed on the side face of the slab. This observation indicates that less transverse load redistribution was activated than in other slab shear experiments. Therefore, the shear stress distribution at the support is more concentrated around the peak load than when more transverse load redistribution is activated. As such, the chosen experiment is a conservative lower bound for the studied case of slab bridges subjected to concentrated and distributed loads.

The experiment has been carried out with a concentrated load representing the wheel print that is used in Load Model 1 of NEN EN 1991-2:2003 [1]. The influence of the size of the concentrated load and on the shear capacity on the shear stress distribution is known [27] . Therefore, the recommended distribution width of $4d_l$ is to be used with concentrated wheel loads of the size as used in Load Model 1 of NEN EN 1991-2:2003 or similar wheel prints.

The shear-span-to-depth ratio used in the experiment is $a/d_l = 2.26$. This short distance ensures that the stress distribution at the support does not differ much from the stress distribution at the cross-section containing the concentrated load. For practical use, the cross-section with the concentrated can thus be analyzed, regardless of the shear span. An additional reason for using $a/d_l = 2.26$ is that this distance closely corresponds to the recommended distance for assessment of reinforced concrete slab bridges, where the first truck is placed at $a_v/d_l = 2.5$ [39].

The reader should note that the presented work is only applicable to solid slab bridges. For floor slabs of buildings or footings, a different behavior can be expected. The behavior of slab bridges is governed by the span direction, while for floor slabs of an even floor plan, both the longitudinal and transverse direction can become equally important. Moreover, the results of the current analysis refer to bridges on line supports or on a closely spaced series of bearings, so that punching of the bearings does not become a governing failure mode. In floor slabs, punching of the columns can become the governing failure mode and influences the flow of shear stresses.

8. Summary and conclusion

The principle of Levels of Approximation, as used in the recently published *fib* Model Code 2010 is applied to assessment of reinforced concrete slab bridges, resulting in Levels of Assessment. Increasing the Level of Assessment means using a computational technique that

requires more time but that gives results that are expected to be more accurate. For the shear assessment of reinforced concrete solid slab bridges, Level of Assessment I is an analysis with the Quick Scan method, a conservative, fast, spreadsheet-based tool that can quickly identify which bridges contain cross-sections that need further study. Level of Assessment II is an analysis in which the shear stress at the support caused by the applied loads is determined with a linear finite element model. The result in the program is a shear stress distribution over the width of the support. As always in finite element models, the peak needs to be smoothed out. This paper analyzed over which width the peak shear stress at the support can be distributed for the shear analysis. Previously, rules of thumb were used for this distribution width. This study quantifies the distribution width for the first time based on experimental evidence.

To study the required distribution width in the finite element model, a comparison is made between an experiment and a linear finite element model. The experiment S25T1 was a test of a reinforced concrete solid slab subjected to a single concentrated load close to the support. The support was equipped with seven load cells to measure the reaction force profile over the width of the support. These elements were used as well in the linear finite element model for this study, in which the slab was modeled with shell elements.

The effect of distributing the peak shear stress over a distance $2d_l$ and $4d_l$ over the support are studied with the experimental results and the results from the finite element model. The analysis showed that a distribution width of $4d_l$ should be used for smoothing out the peak shear stress found in a linear finite element program. When the Unity Check of the experiment is calculated, the large inherent conservativism of both the Level of Assessment I and Level of Assessment II is seen.

Finally, a case study is carried out, in which the application of Level of Assessment I and Level of Assessment II is studied, and it is found that the approach with the Levels of Assessment works, since Level of Assessment I gives a more conservative Unity Check than Level of Assessment II.

Acknowledgements

The authors wish to express their gratitude and sincere appreciation to the Dutch Ministry of Infrastructure and the Environment (Rijkswaterstaat) for financing this research work.

List of notation

a	center-to-center distance between the load and the support
a_v	face-to-face distance between the load and the support
d_l	effective depth to the longitudinal reinforcement
$f_{c,cube}$	cube compressive strength of the concrete
f_{ck}	characteristic concrete cylinder compressive strength
f_{ct}	cube splitting strength of concrete
f_{ym}	yield strength of steel
f_{um}	ultimate tensile strength of steel
h	height
k	size effect factor
s	displacement
t	time
v_{Ed}	governing shear stress in cross-section from the applied loads
v_{min}	lower bound for shear capacity

$v_{Rd,c}$	shear capacity of cross-section as prescribed by NEN-EN 1992-1-1:2005 [2]
x	position along the width of the slab
F	applied load
F_i	measured force on the prestressing bars, with *i* the number of the bar (1, 2 or 3).
F_{max}	maximum concentrated load in the experiment
$F_{tot,2d}$	total applied reaction force over $2d_l$
$F_{tot,4d}$	total applied reaction force over $4d_l$
P_u	maximum applied load in experiment
UC	Unity Check value
V_{min}	minimum shear capacity
ρ_l	longitudinal reinforcement ratio
ρ_t	transverse reinforcement ratio
τ_{2d}	resulting shear stress over $2d_l$
τ_{4d}	resulting shear stress over $4d_l$

References

[1] CEN. Eurocode 1: Actions on structures - Part 2: Traffic loads on bridges, NEN-EN 1991-2:2003. Brussels, Belgium: Comité Européen de Normalisation; 2003. p. 168.

[2] CEN. Eurocode 2: Design of Concrete Structures - Part 1-1 General Rules and Rules for Buildings. NEN-EN 1992-1-1:2005. Brussels, Belgium: Comité Européen de Normalisation; 2005. p. 229.

[3] Dutch Institute for Normalization. NEN 3880:1974 Provisions Concrete. 1974.

[4] Dutch Institute for Normalization. NEN 1009:1962 Provisions Reinforced Concrete. 1962.

[5] Walraven JC. Residual shear bearing capacity of existing bridges. fib Bulletin 57, Shear and punching shear in RC and FRC elements; Proceedings of a workshop held on 15-16 October 2010. Salò, Lake Garda, Italy2010. p. 129-38.

[6] Lantsoght EOL, van der Veen C, de Boer A, Walraven J. Transverse Load Redistribution and Effective Shear Width in Reinforced Concrete Slabs. Heron. in press:29 pp. .

[7] Lantsoght EOL, van der Veen C, De Boer A, Walraven J. Influence of Width on Shear Capacity of Reinforced Concrete Members. ACI Structural Journal. 2014;111:1441-50.

[8] Lantsoght EOL, Van der Veen C, Walraven JC, De Boer A. Transition from one-way to two-way shear in slabs under concentrated loads. Magazine of Concrete Research. 2015;67:909-22.
[9] Lantsoght EOL, Van der Veen C, Walraven JC, De Boer A. Database of wide concrete members failing in shear. Magazine of Concrete Research. 2015;67:33-52.
[10] Regan PE. Shear Resistance of Concrete Slabs at Concentrated Loads close to Supports. London, United Kingdom: Polytechnic of Central London; 1982. p. 24.
[11] Furuuchi H, Takahashi Y, Ueda T, Kakuta Y. Effective width for shear failure of RC deep slabs. Transactions of the Japan concrete institute. 1998;20:209-16.
[12] Richart FE, Kluge RW. Tests of reinforced concrete slabs subjected to concentrated loads; a report of an investigation. University of Illinois Engineering Experiment Station Bulletin No 314. Urbana: University of Illinois; 1939. p. 86.
[13] Graf O. Experiments on the Capacity of Reinforced Concrete Slabs under a concentrated Load close to a Support. Deutscher Ausschuss für Eisenbeton. 1933;73:10-6.
[14] fib. Model code 2010: final draft. Lausanne: International Federation for Structural Concrete; 2012.
[15] Lantsoght EOL, van der Veen C, Walraven JC. Shear assessment of solid slab bridges. In: Dehn F, Moyo P, editors. ICCRRR 2012, 3rd International Conference on Concrete Repair, Rehabilitation and Retrofitting. Cape Town, South Africa2012. p. 827-33.
[16] Vergoossen R, Naaktgeboren M, 't Hart M, De Boer A, Van Vugt E. Quick Scan on Shear in Existing Slab Type Viaducts. International IABSE Conference, Assessment, Upgrading and Refurbishment of Infrastructures. Rotterdam, The Netherlands2013. p. 8.
[17] Walraven JC. Minimum shear capacity of reinforced concrete slabs without shear reinforcement: the value v_{min}. 2013. p. 20 (in Dutch).
[18] Lantsoght EOL, Van der Veen C, Walraven J, De Boer A. Recommendations for the Shear Assessment of Reinforced Concrete Solid Slab Bridges. IABMAS 2014. Shanghai, China2014.
[19] Lantsoght EOL, van der Veen C, Gijsbers FBJ. Achtergrondrapport bij spreadsheet voor toetsing aan rand. Delft University of Technology; 2012. p. 50.
[20] Rijkswaterstaat. Guidelines for Nonlinear Finite Element Analysis of Concrete Structures. 2012. p. 65.
[21] Belletti B, Damoni C, Hendriks MAN, de Boer A. Analytical and numerical evaluation of the design shear resistance of reinforced concrete slabs. Structural Concrete. 2014;15:317-30.
[22] Koekkoek RT, Lantsoght EOL, Hordijk DA. Proof loading of the ASR-affected viaduct Zijlweg over highway A59. Delft, The Netherlands: Delft University of Technology; 2015. p. 180.
[23] Lantsoght EOL. Ruytenschildtbrug: Analyse proefresultaten uiterste grenstoestand. Delft, The Netherlands: Delft University of Technology; 2015. p. 89.
[24] Koekkoek RT, Lantsoght EOL, Yang Y, Hordijk DA. Analysis report for the assessment of Viaduct De Beek by Proof Loading. Delft, The Netherlands: Delft University of Technology; 2016. p. 125.
[25] Fennis SAAM, van Hemert P, Hordijk D, de Boer A. Proof loading Vlijmen-Oost; Research on assessment method for existing structures (in Dutch). Cement. 2014;5:40-5.
[26] Fennis SAAM, Hordijk DA. Proefbelasting Halvemaansbrug Alkmaar. Delft, The Netherlands: Delft University of Technology; 2014. p. 72.
[27] Lantsoght EOL, van der Veen C, Walraven JC. Shear in One-way Slabs under a Concentrated Load close to the support. ACI Structural Journal. 2013;110:275-84.

[28] Lantsoght EOL, van der Veen C, De Boer A, Walraven J. One-way slabs subjected to a combination of loads failing in shear. ACI Structural Journal. 2015;112:419-28.
[29] Prochazkova Z, Lantsoght EOL. Material properties – Felt and Reinforcement For Shear test of Reinforced Concrete Slab. Delft University of Technology; 2011. p. 28.
[30] Lantsoght EOL. Tests of reinforced concrete slabs subjected to a line load and a concentrated load. Delft University of Technology; 2012. p. 271.
[31] TNO DIANA. Users Manual of DIANA, Release 9.4.4. Delft, The Netherlands2012.
[32] Rijkswaterstaat. Validating the Guidelines for Nonlinear Finite Element Analysis of Concrete Structures. in press. p. 187.
[33] Belletti B, Damoni c, Hendriks MAN, Den Uijl JA. Nonlinear finite element analyses of reinforced concrete slabs: comparison of safety formats. In: Van Mier JGM, Ruiz G, Andrade C, Yu RC, Zhang XX, editors. VIII International Conference on Fracture Mecahnics of concrete and Concrete Structures, FraMCoS-82013. p. 12.
[34] Cantone R, Belletti B, Muttoni A, Ruiz MF. APPROACHES FOR SUITABLE MODELLING AND STRENGTH PREDICTION OF REINFORCED CONCRETE SLABS. In: Beushausen H, editor. fib Symposium 2016, Performance-based approaches for concrete structures. Cape Town, South Africa2016. p. 8.
[35] Lantsoght EOL, van der Veen C, de Boer A. Plastic model for asymmetrically loaded reinforced concrete slabs. ACI SP Recent developments on slabs. in press:21.
[36] Lantsoght EOL, De Boer A, Van der Veen C. Levels of Approximation for the shear assessment of reinforced concrete slab bridges. Structural Concrete. 2017;18:143-52.
[37] Lantsoght EOL, Van der Veen C, De Boer A, Hordijk DA. Proof load testing of reinforced concrete slab bridges in the Netherlands. Structural Concrete. in press:29.
[38] Steenbergen RDJM, Vervuurt AHJM. Determining the in situ concrete strength of existing structures for assessing their structural safety. Structural Concrete. 2012;13:27-31.
[39] Lantsoght EOL, van der Veen C, de Boer A, Walraven JC. Recommendations for the Shear Assessment of Reinforced Concrete Slab Bridges from Experiments Structural Engineering International. 2013;23:418-26.

List of tables and figures

List of Tables:

List of Figures:

Fig. 9 – Distribution of the shear stress over the support obtained from the finite element model. Dashed lines show $2d_l$ and $4d_l$ around the peak of the shear stress distribution, and full lines show these distances around the center of the slab.

Fig. 10 – Stress-strain curve for concrete to be used in non-linear finite element model [32].

Fig. 11 – Stress-strain curve for reinforcement steel of diameter 20 mm to be used in non-linear finite element model [32].

Fig. 12 – Example of crack strains at peak load for a strip of a slab, isolated from the full model to analyze the crack strains [32].

Table 1- Comparison between the results from the experiment and the results from the finite element analysis.

Concentrated load	585 kN		1314 kN	
Shear stress	τ_{2d} (MPa)	τ_{4d} (MPa)	τ_{2d} (MPa)	τ_{4d} (MPa)
Measurements	1.51	0.87	4.13	2.63
Model, integrating stresses	1.30	1.10	3.28	2.70
Model, reaction forces	1.39	1.27	3.25	2.60

Figure 1
Click here to download Figure: fig 1.eps

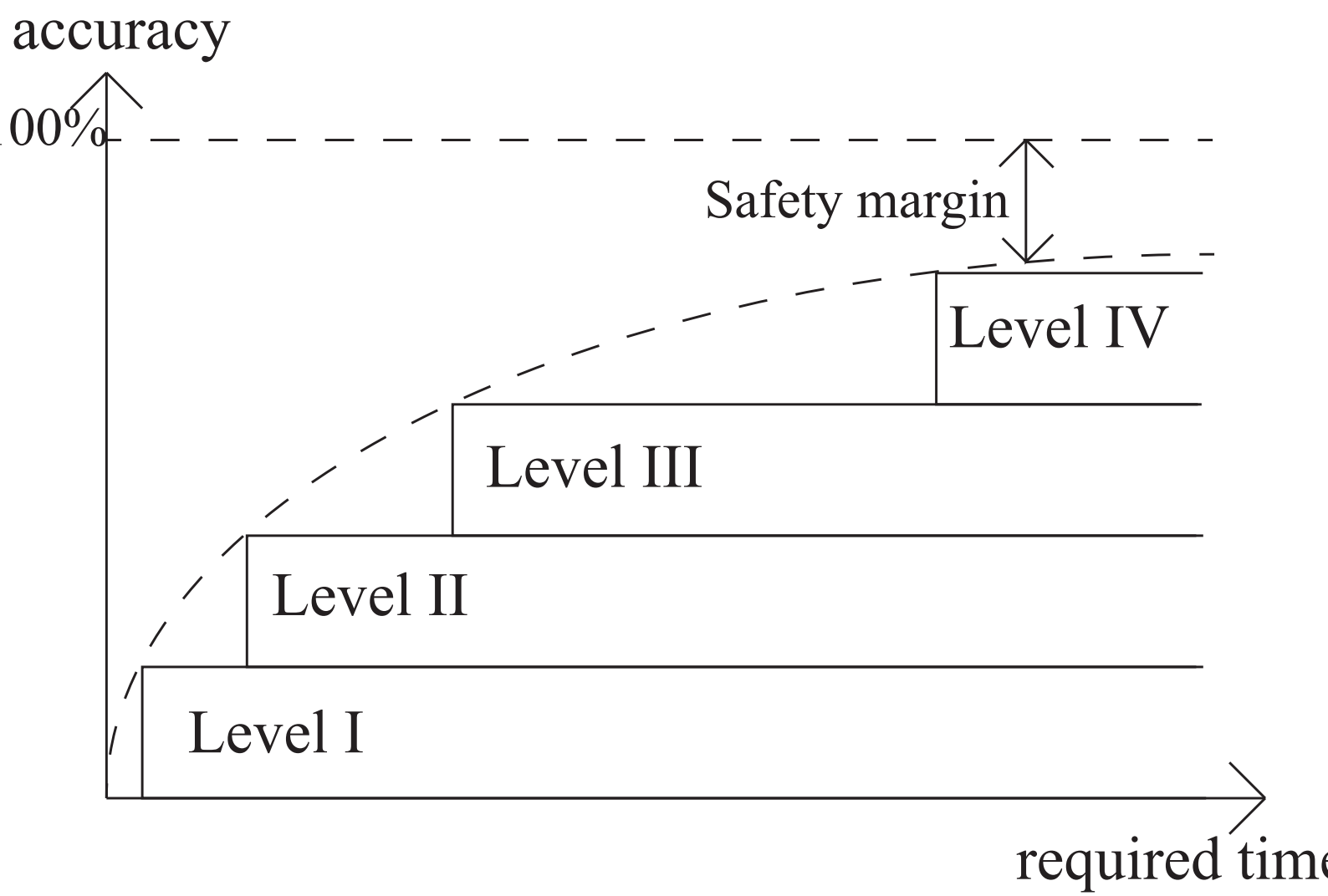

Figure 2
Click here to download Figure: fig 2.eps

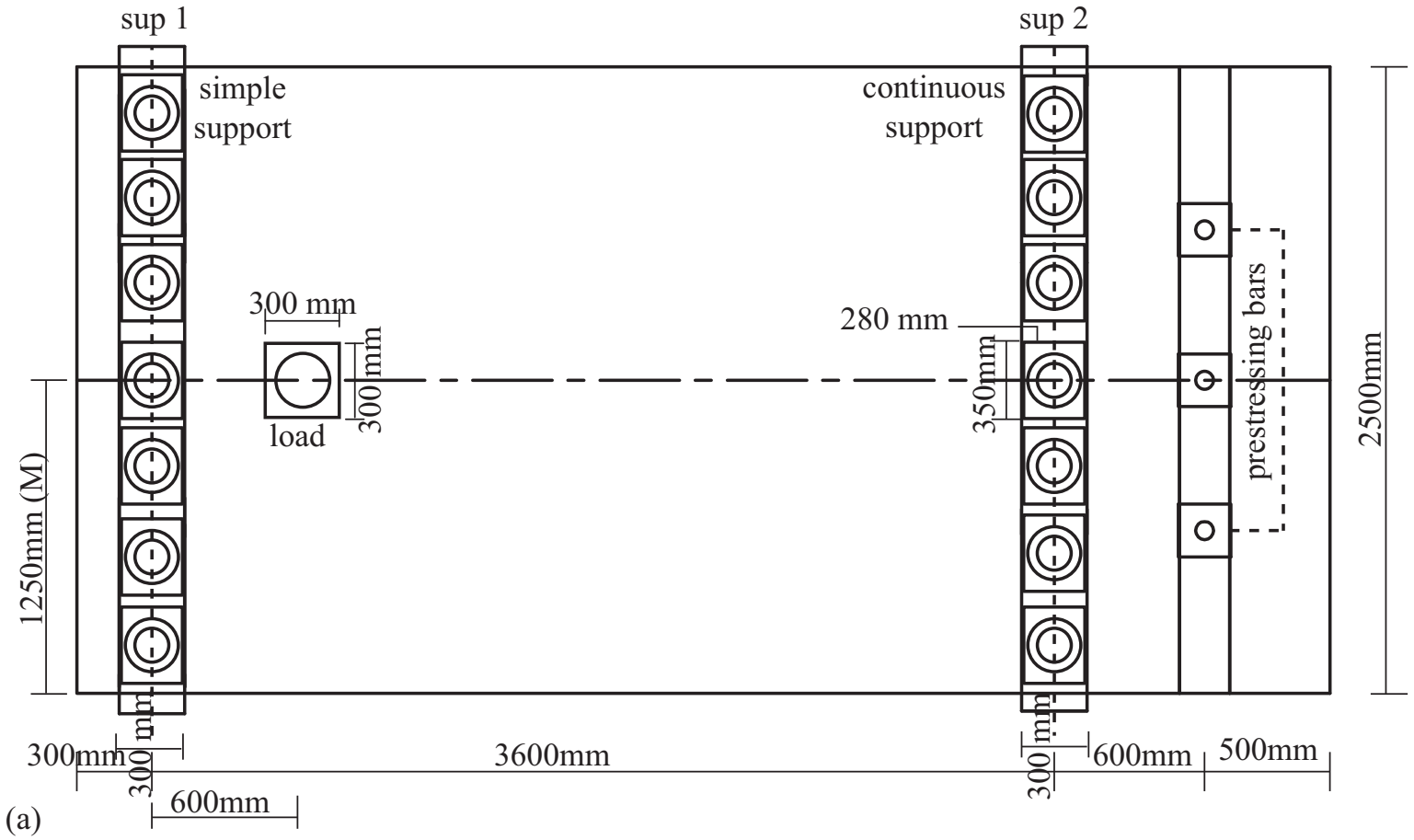

(a)

b)

Figure 3
Click here to download Figure: fig 3.eps

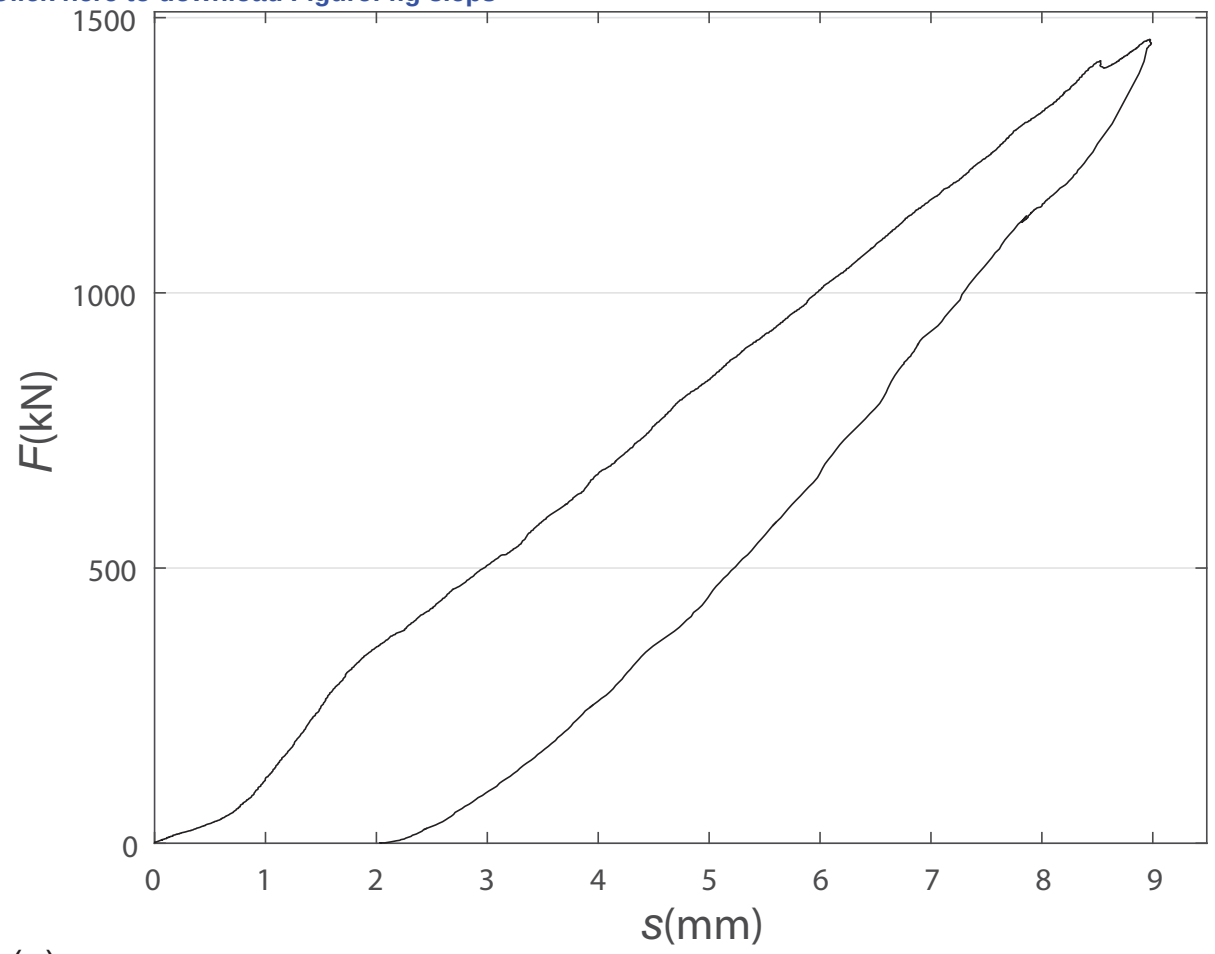

(a)

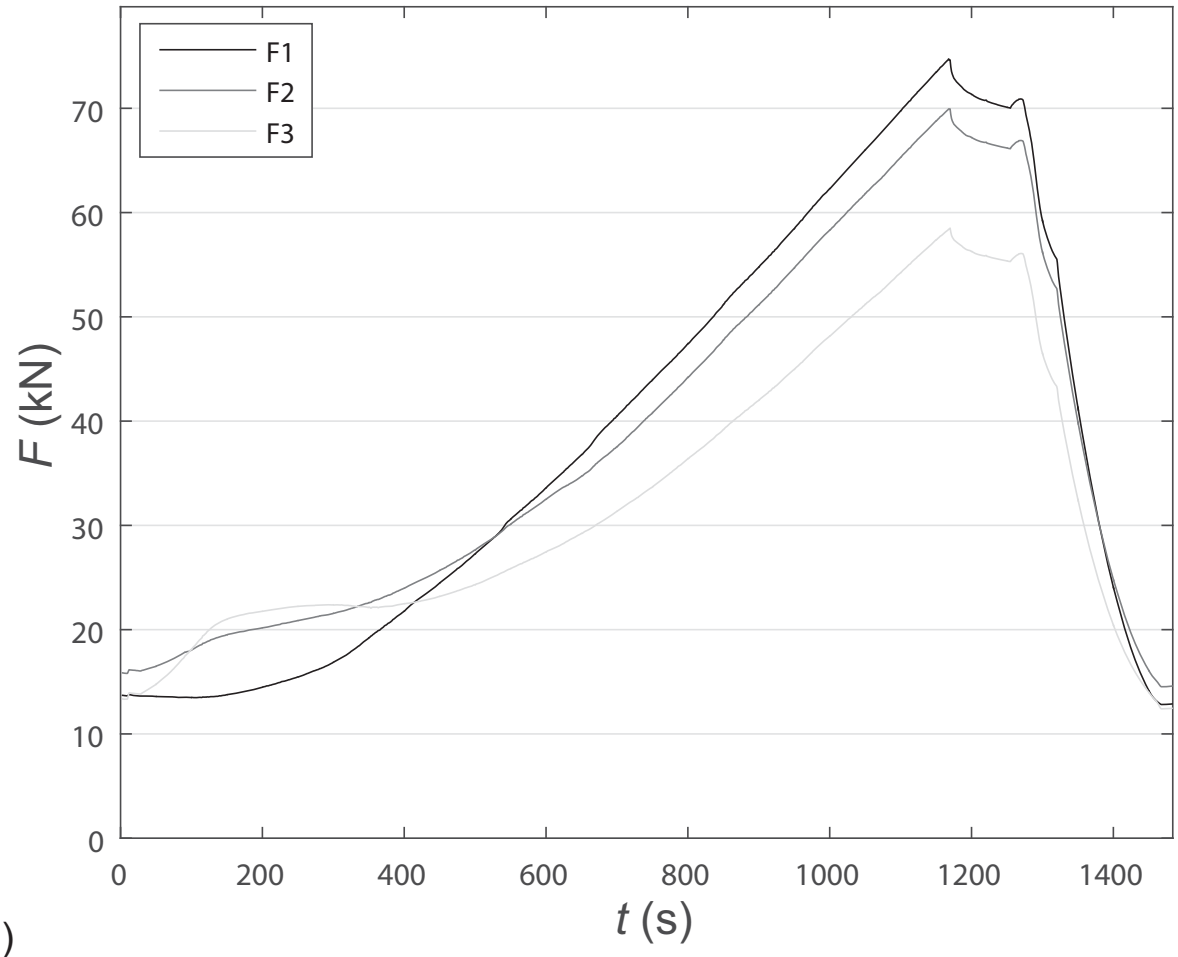

(b)

Figure 4
Click here to download Figure: fig 4.eps

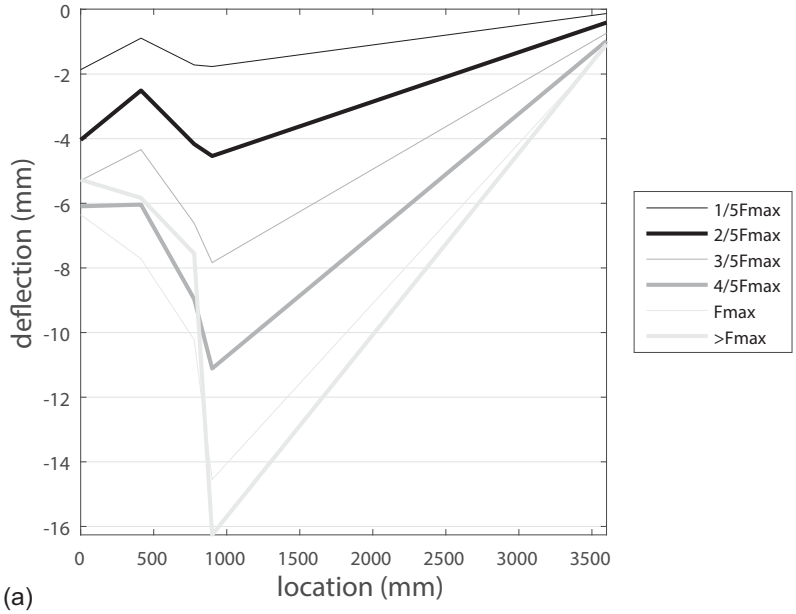

(a)

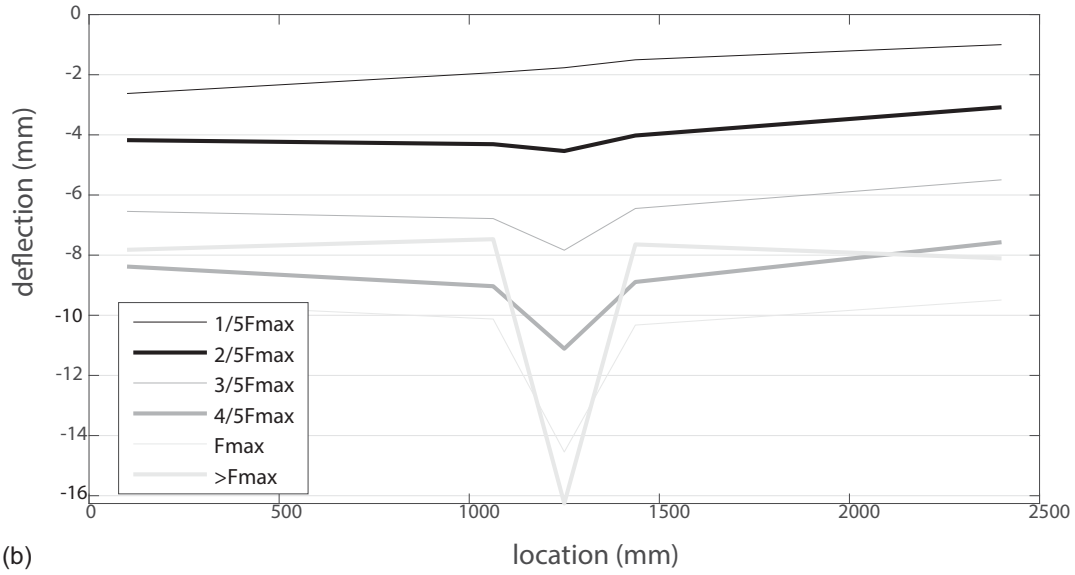

(b)

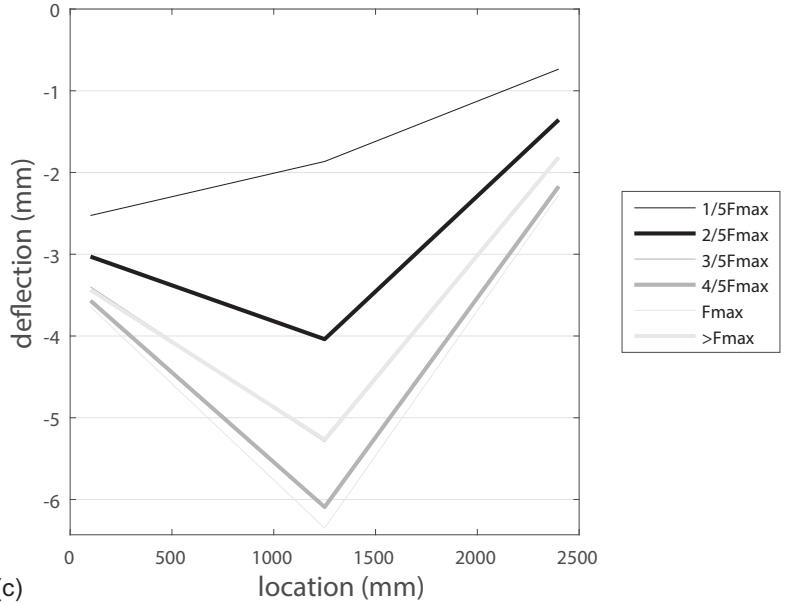

(c)

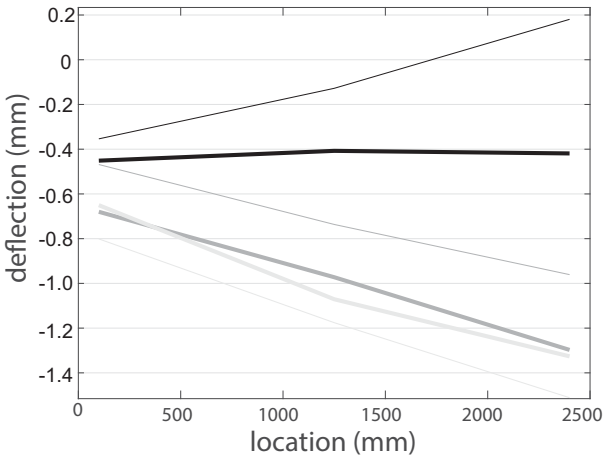

(d)

Figure 5
Click here to download Figure: fig 5.eps

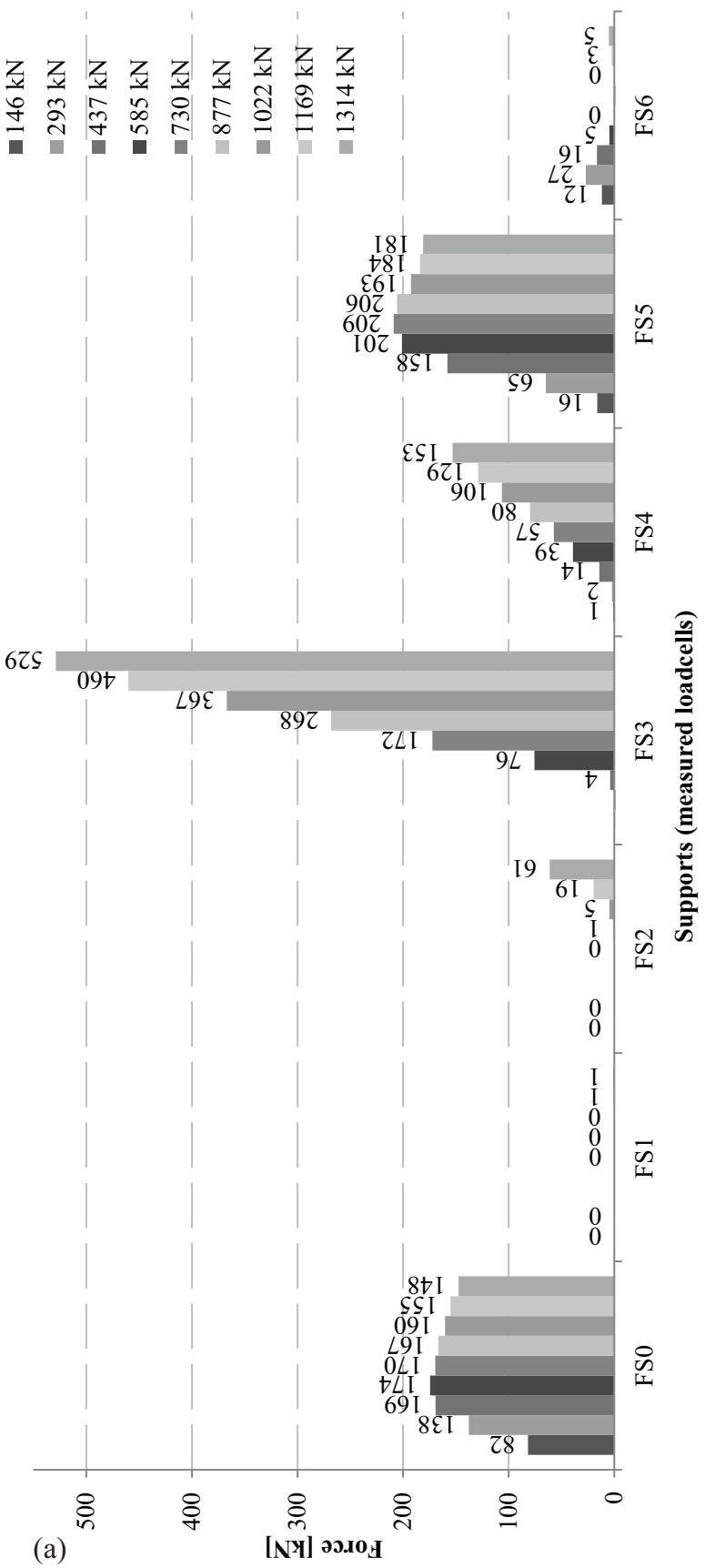

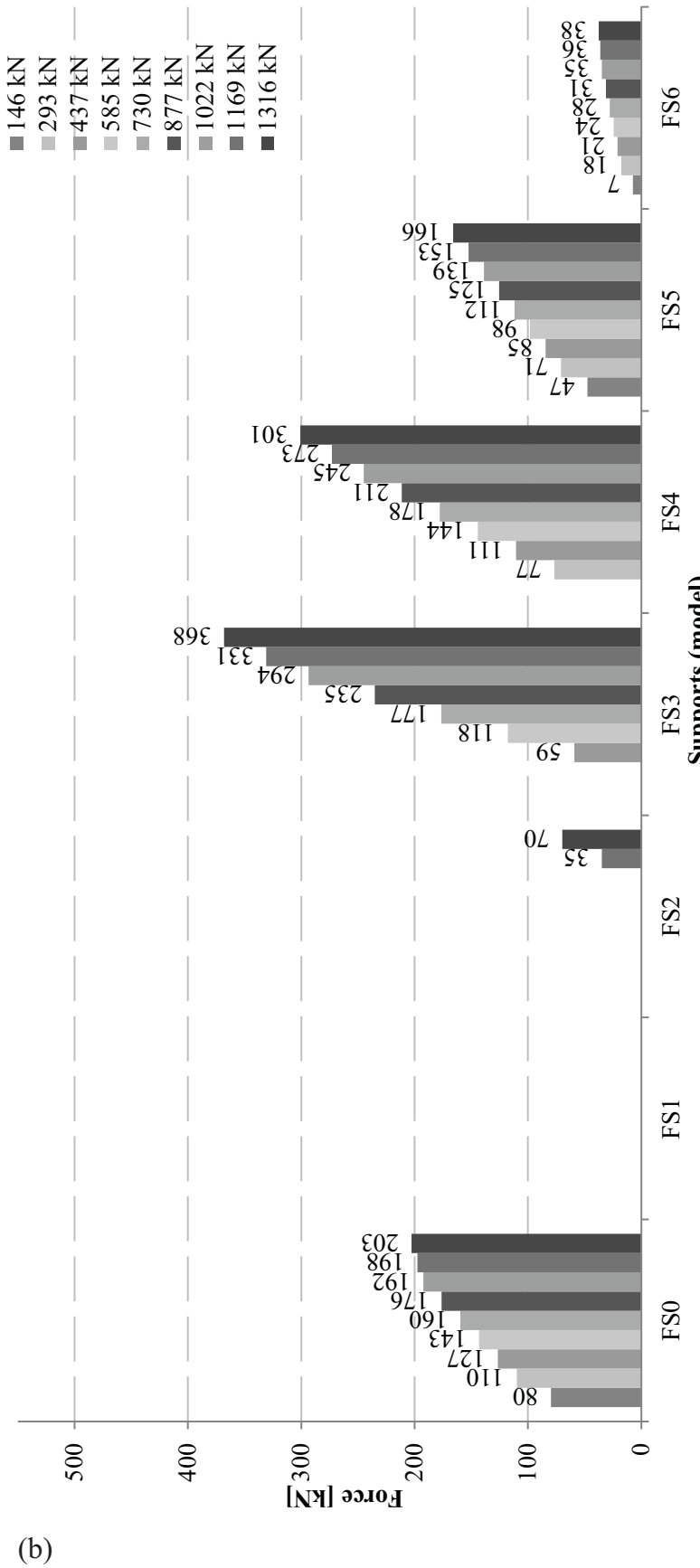

Figure 6
Click here to download Figure: fig 6.eps

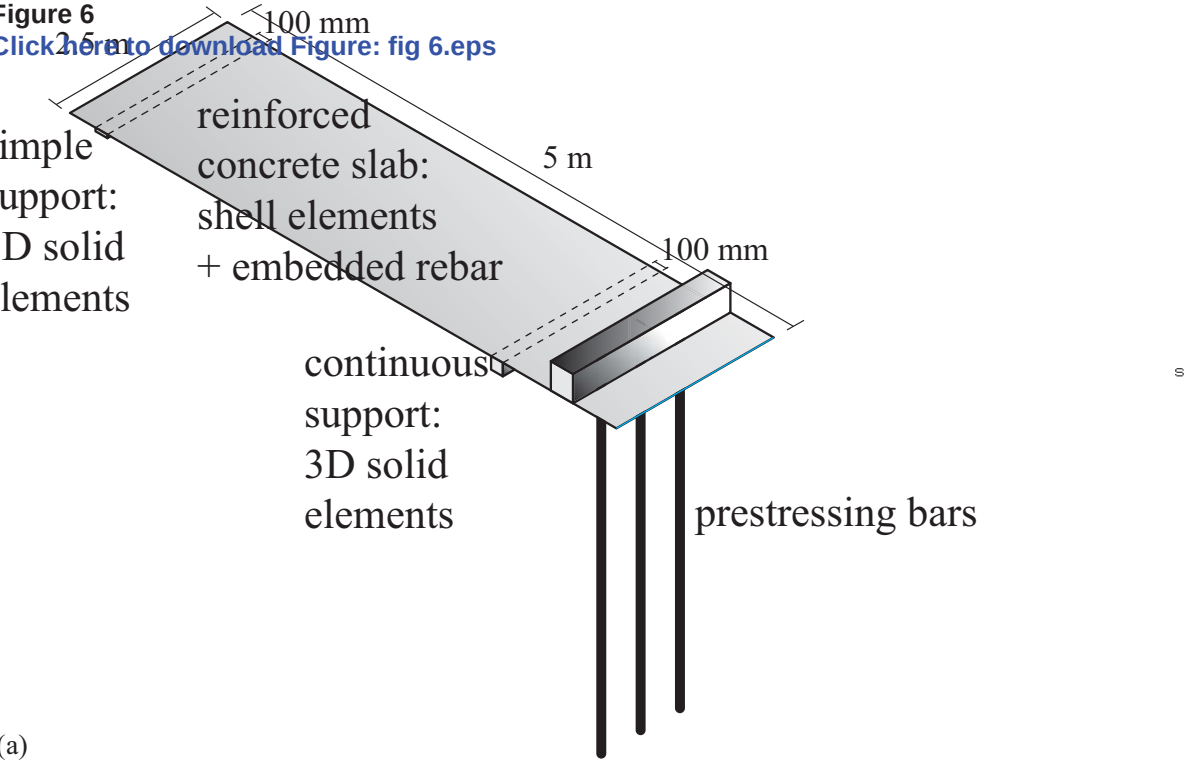

(a)

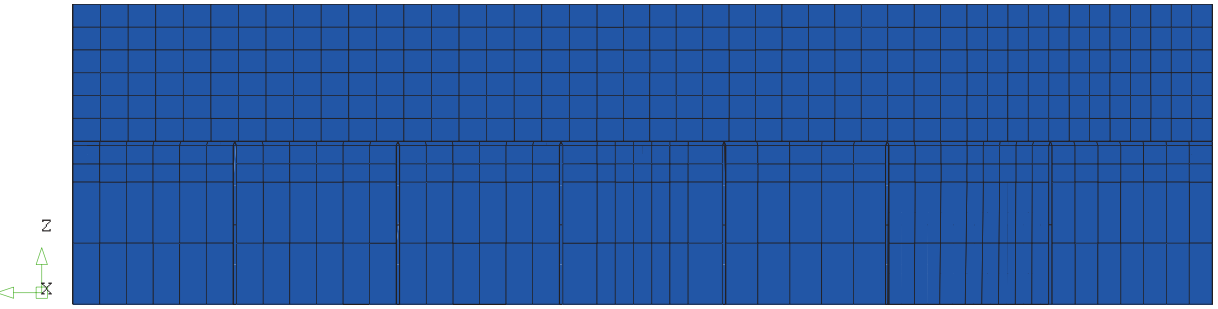

(b)

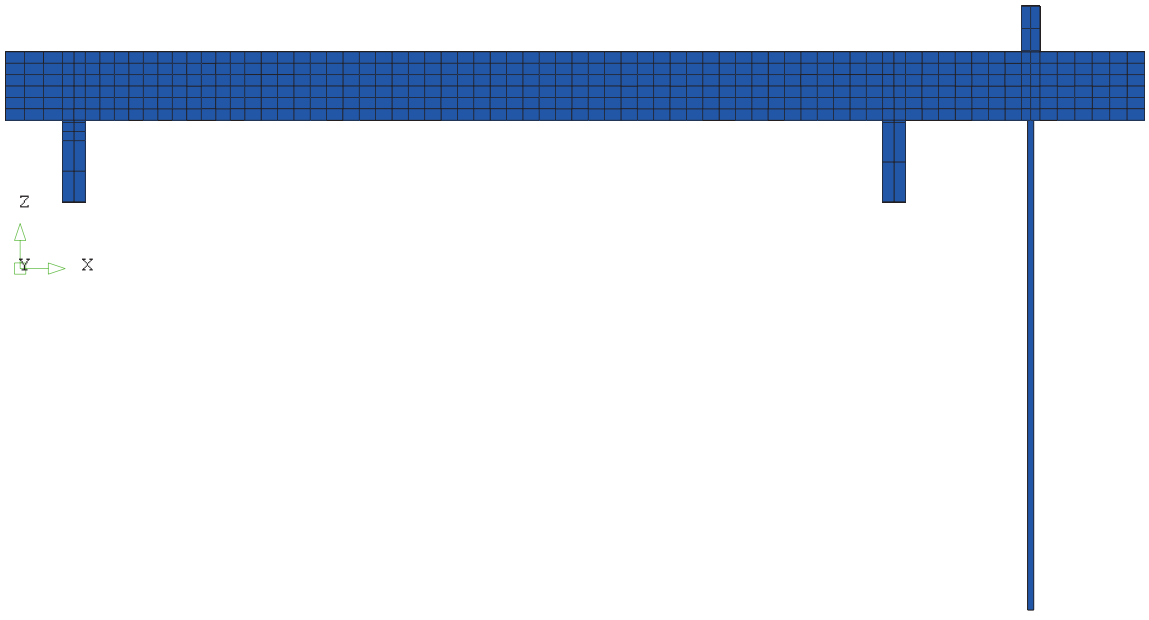

(c)

Figure 7
Click here to download Figure: fig 7.eps

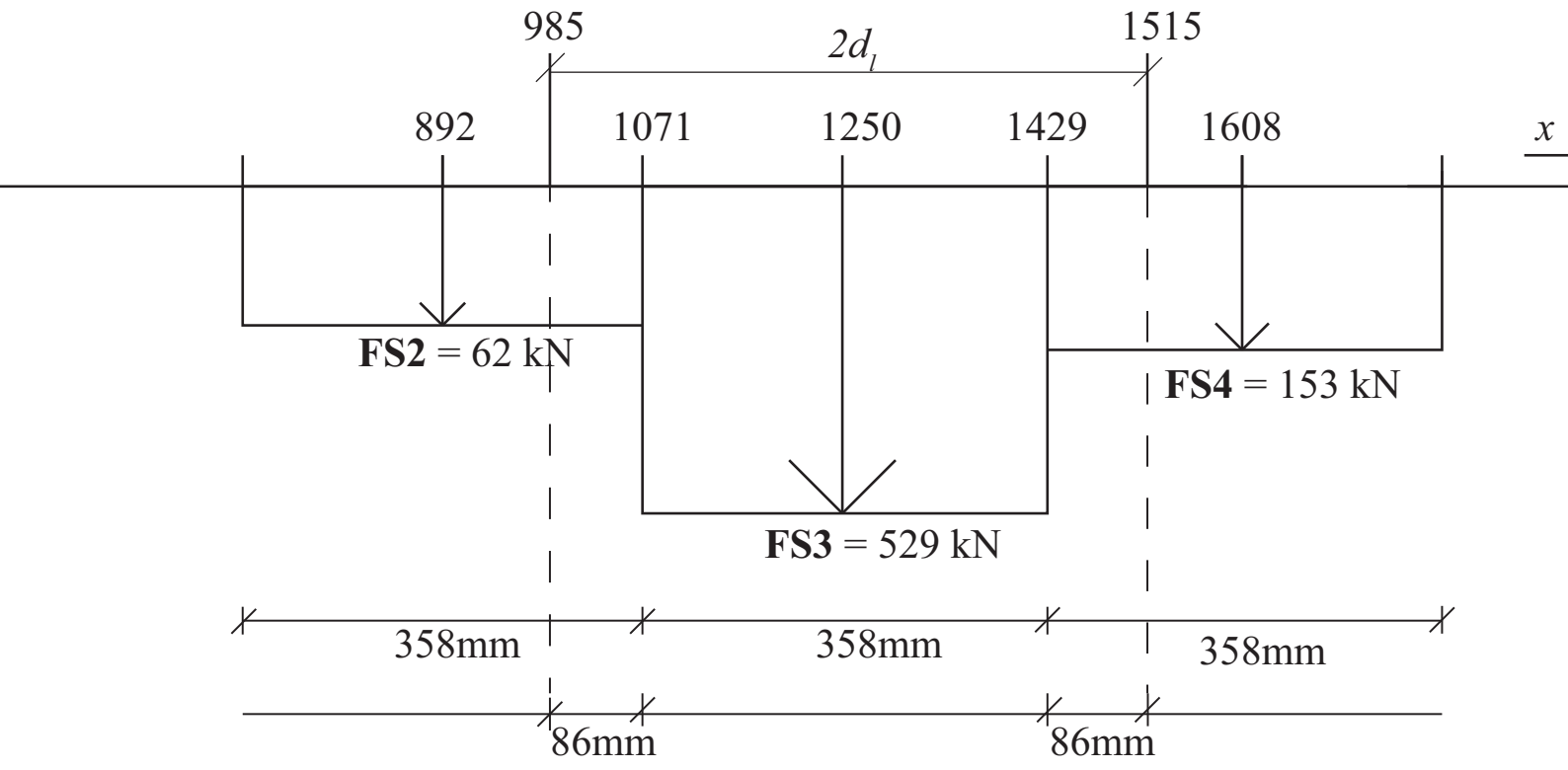

Figure 8
Click here to download Figure: fig 8.eps

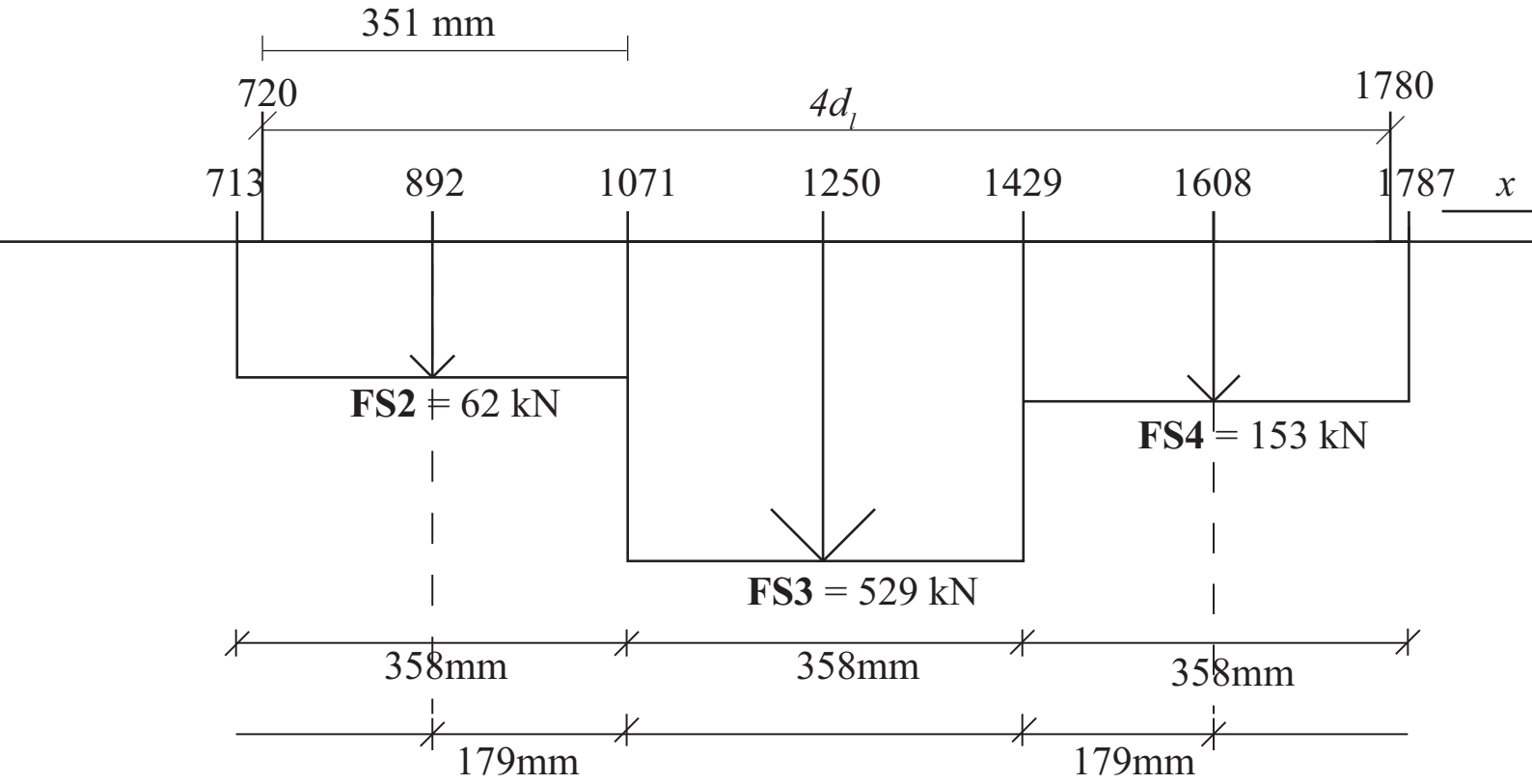

Figure 9
Click here to download Figure: fig 9.eps

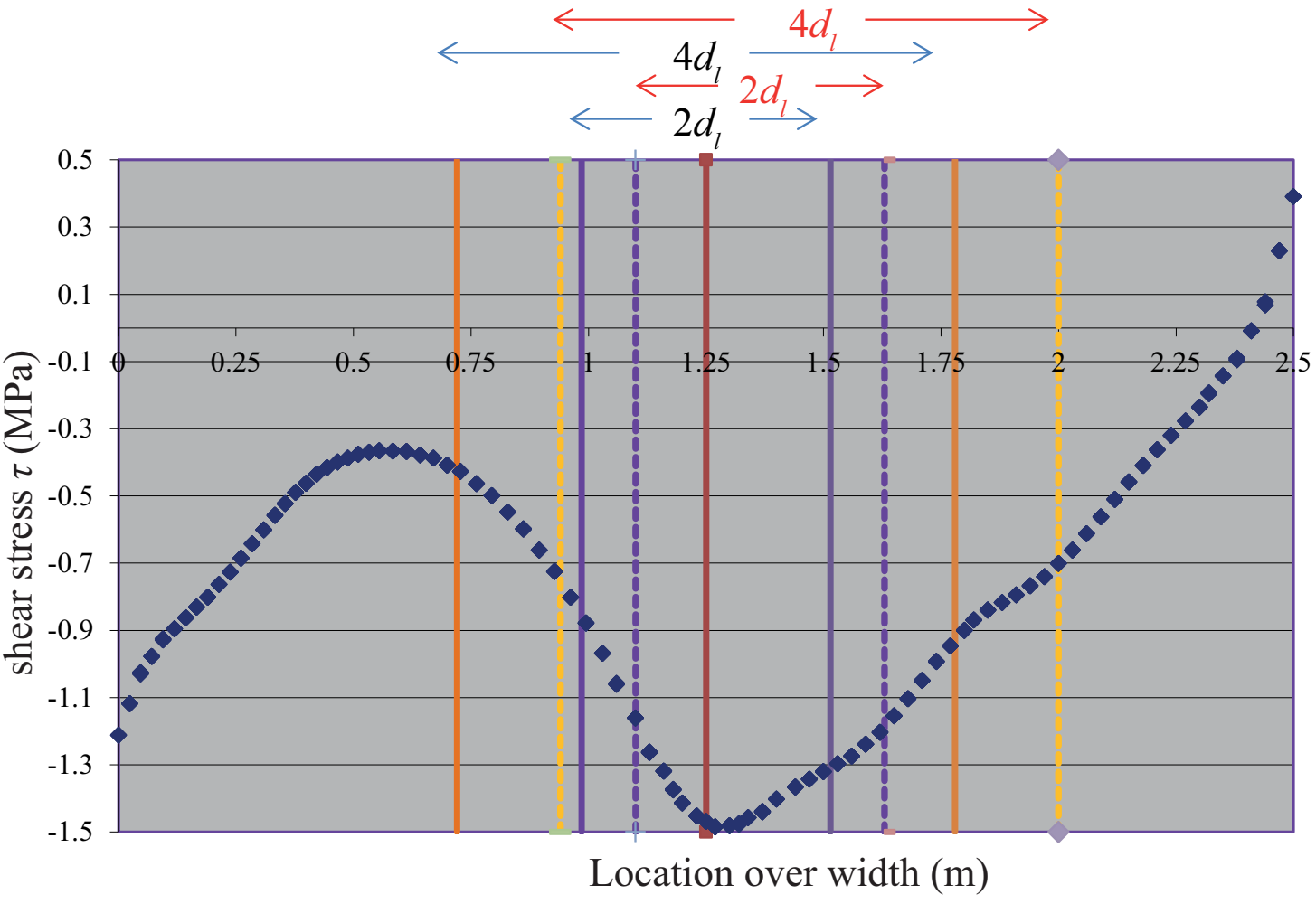

Figure 10

Click here to download high resolution image

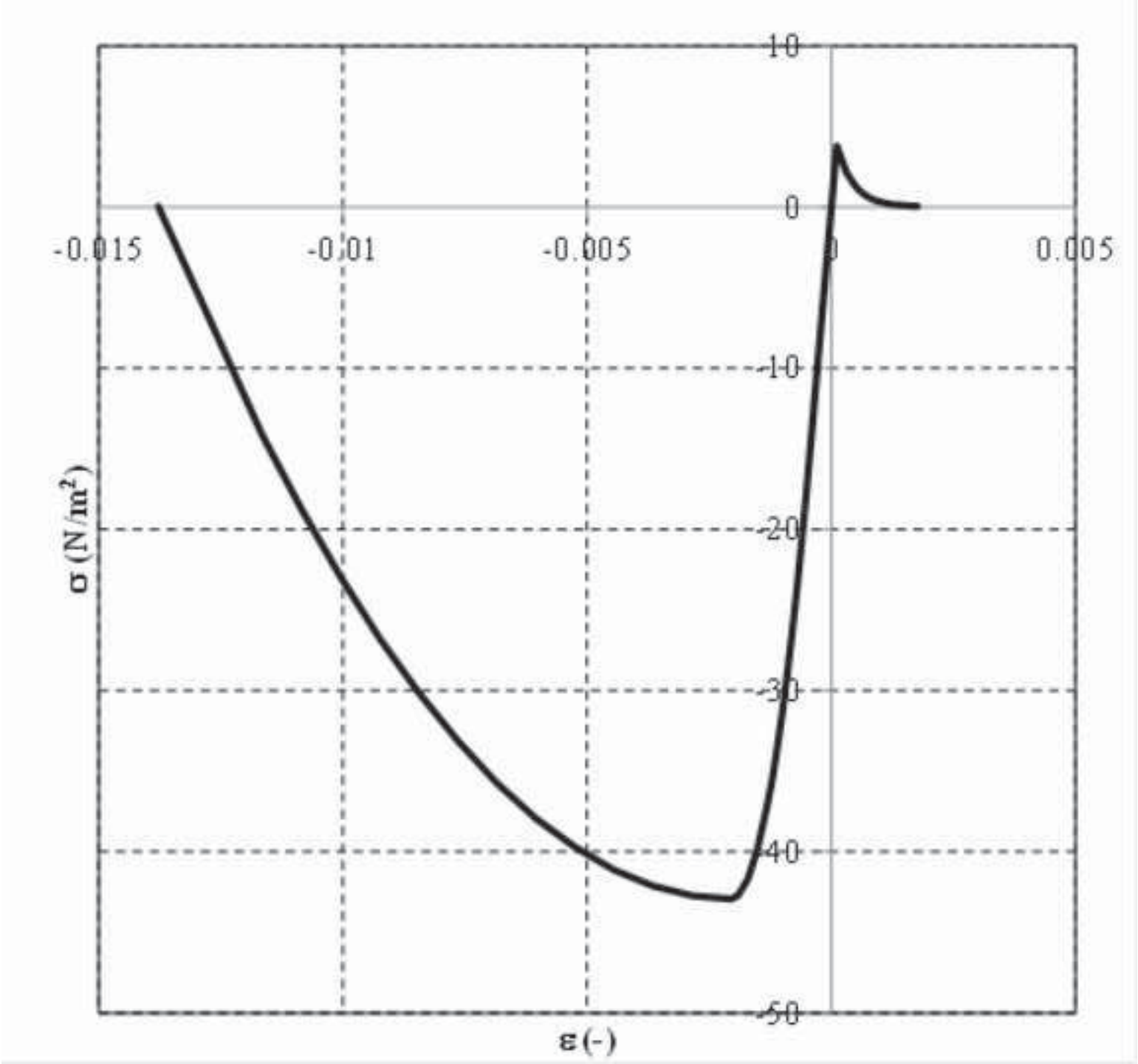

Figure 11

Click here to download high resolution image

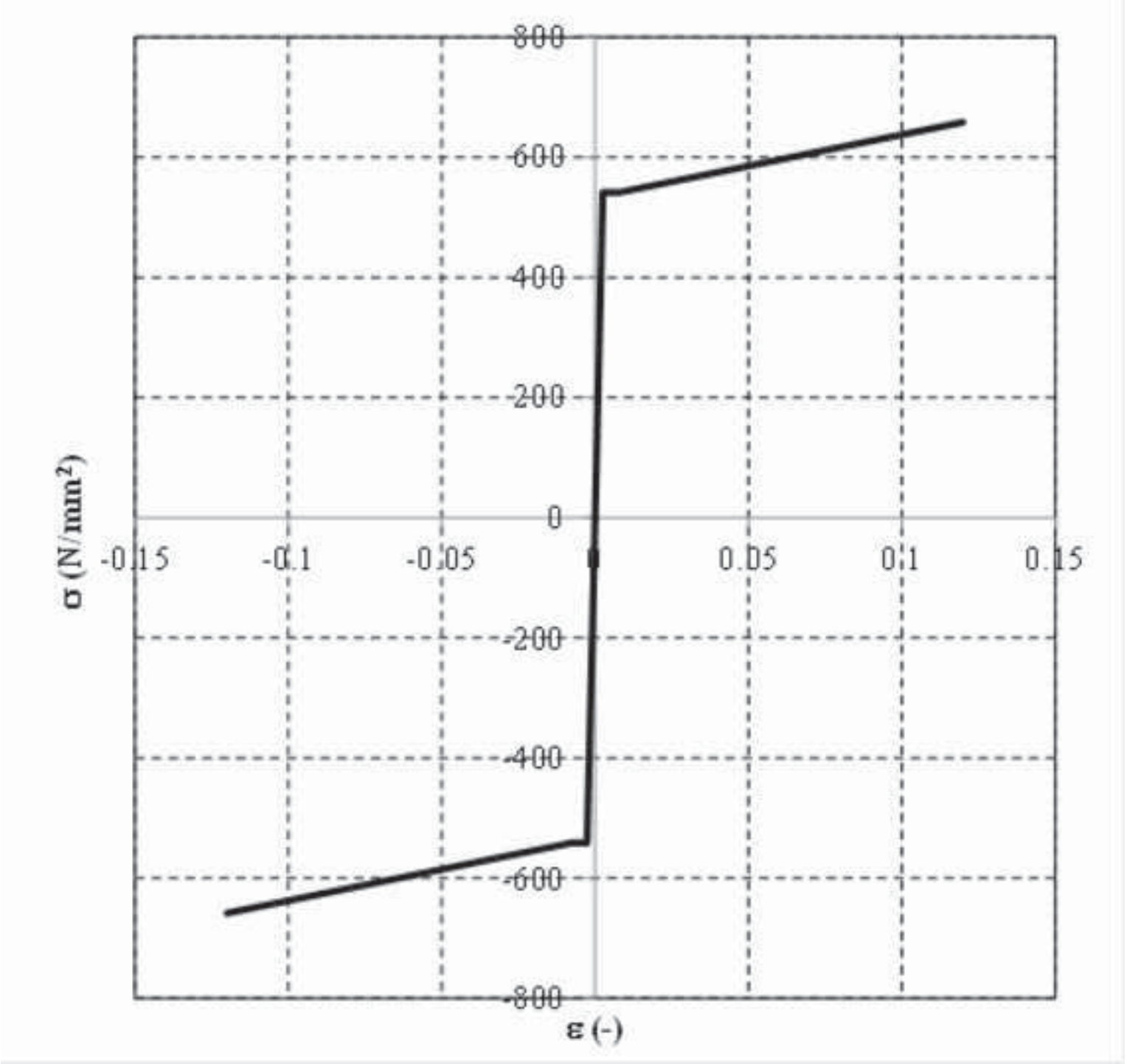

Figure 12

Click here to download high resolution image